Available online at www.sciencedirect.com
SCIENCE DIRECT®
Journal of Marine Systems 44 (2004) 107–124
JOURNAL OF MARINE SYSTEMS
www.elsevier.com/locate/jmarsys

The cause of Barents Sea biomass dynamics

Harald Yndestad*

Aalesund University College, N-6025 Aalesund, Norway

Received 8 October 2002; accepted 15 August 2003

Abstract

The fluctuations of the biomasses in the Barents Sea have been poorly understood and caused problems in biomass management. Better long-term forecasting is thus crucial for an economical and sustainable utilization of the biomass.

The present paper presents a wavelet analysis of the Kola temperature series and the biomass time series of Barents Sea Shrimp (*Pandalus borealis*), Barents Sea capelin (*Mallotus villosus*), Norwegian spring spawning herring (*Clupea harengus*), Northeast Arctic cod (*Gadus morhua*), and Northeast Arctic haddock (*Melanogrammus aeglefinus*). The wavelet shows a close relation between the 18.6-year lunar nodal tide and dominant temperature cycles in the Kola temperature series. It also shows that all biomass time series are correlated to dominant cycles of 18.6/3 = 6.2, 18.6 and 3∗18.6 = 55.8 years in the Kola section. This indicates that fluctuations of the temperature and the biomass in the Barents Sea are a deterministic process caused by the lunar nodal cycle.

The close relation to the stationary 18.6-year lunar tide opens new possibilities for better forecasting and long-term management. The deterministic relation between biomass growth and the Kola cycles opens a possibility of more optimal management in short-term periods of 6 years, medium-term management of 18 years and long-term management of 55–75 years. The stationary biomass cycles can be represented by a simple phase-clock which indicates the current state of the biomass. This method represents a new possibility of long-term biomass forecasting.

Keywords: 18.6-year lunar tide; Biomass dynamics; Barents Sea; Forecasting; Wavelet analysis

1. Introduction

The Barents Sea has some of the most productive biomasses in the world. During centuries, these biomasses have been of vital importance for settlement and economic growth in the western part of Norway. Some years, the biomass influx is abundant and some years the influx may be insufficient in relation to the demand. People dependent on fishing have always known that the biomass stock has a short time and long time fluctuation. These fluctuations have been explained by migrations, climate change, predators, introduction of new fishing equipment and more. When the marine research started at the beginning of the last century, the main task was to uncover how nature influenced the stock biomass and the impact of fluctuation on people living by fishing (Rollefsen et al., 1949). Better forecasting in a time span of 5–10 years will be crucial for better planning of an economical and sustainable biomass in the Barents Sea.

A long-term biomass management is based on the theory that if we are able to forecast the biomass

* Tel.: +47-70-16-12-00; fax: +47-70-16-13-00.
E-mail address: Harald.Yndestad@hials.no (H. Yndestad).

0924-7963/$ - see front matter © 2003 Elsevier B.V. All rights reserved.
doi:10.1016/j.jmarsys.2003.08.004

dynamics, then we may control the biomass. To forecast a future biomass, the biomass dynamics has to be deterministic and we need a scientific framework to describe expected biomass fluctuations. System dynamics in nature may be modeled as a holistic approach or as autonomous dynamic systems. The Aristotle (384–322 BC) 'principle of motion and change' represents a holistic approach on systems dynamics. He argued that the causes of movements in nature were a result of a history of chain of movements, that may be traced backwards to the motion of the Sun, the Moon and the stars. In modern science, we may call this approach a domino theory or Earth system science.

Isaac Newton (1642–1727) introduced the mathematical framework of system dynamics by the differential equation $dx/dt = Ax(t)$. From this simple equation, the future state $x(t)$ may be computed when the parameter A and the initial condition $x(0)$ are known. In biomass modeling, $x(t)$ represents the biomass state vector, and the system matrix A represents parameters of recruitment rates, maturing rates, growth rates and mortality rates. Introducing a quota vector $u(t)$, we have the biomass management model $dx/dt = Ax(t) + u(t)$. The biomass is managed by the control law $u(t) = Fx(t)$, where F is the catch rate. By this simple model, we may predict how a quota $u(t)$ may influence the biomass state $x(t)$ in the future. A management model opens a possibility of computing an optimum quota $u(t)$, a sustainable biomass $x(t)$, and biological reference points related to the catch rate F. According to this approach, we may forecast the biomass dynamics as an autonomous system, but at the same time, we have little room for a holistic understanding of long-term biomass dynamics.

In the Barents Sea, there is a predator and prey relation between spices in the biomass. A mutual relation between species introduces a time variant growth model. To overcome this problem, we have to introduce the augmented time variant model $dx/dt = A(t)x(t) + u(t)$ where all interacting species are represented. A time variant dynamic system implies that the new biomass state $x(t)$ and the parameters $A(t)$ have no stationary mean value. No stationary mean growth matrix implies that forecasting is dependent on the initial value $x(0)$, there is no stationary optimum quota $u(t)$, no stable biomass $x(t)$, and no stationary biological reference points of F. Each species in the Barents Sea is still dependent on a food chain outside the model, which is dependent on the ocean dynamic and the climate dynamics. In other words, the more this model is augmented, the more the model is moving into the holistic approach from Aristotle.

The biomass fluctuations in the Barents Sea may be more or less influenced by the autonomous biomass dynamics, interactions between the species, fishing activity, and a more complex dynamic chain that may be traced back to the movement of the Earth and the Moon. In this investigation, the Kola section temperature series, the biomass of Northeast Arctic shrimp (*Pandalus borealis*), Barents Sea capelin (*Mallotus villosus*), Norwegian Spring spawning herring (*Clupea harengus*), Northeast Arctic cod (*Gadus morhua*), and Northeast Arctic haddock (*Melanogrammus aeglefinus*) are analysed. The time series are analysed by a wavelet transformation to identify the cycle time and phase of the dominant fluctuations. The analysis has identified a close relation to the 18.6-year lunar cycle in all time series.

The identified dominant cycles of about 18.6, $18.6/3 = 6.2$, and $3*18.6 = 55.8$ years in the Kola time series indicated that Atlantic inflow to the Barents Sea is influenced by long-term tides. When the same cycles are identified in the analysed biomasses, it indicates that cycles of Atlantic inflow influence the food chain and biomass growth in the Barents Sea. Since the fluctuations are related to deterministic periods of 6.2, 18.6 and 55.8 years, the cycle vectors may be visualized by a phase-clock. In biomass forecasting, this phase-clock is an indicator of when we may expect changes in the biomass fluctuations.

2. Materials and methods

2.1. Materials

Russian scientists at the PINRO institute in Murmansk have provided monthly temperature values from the upper 200 m in the Kola section along the 33°30′E meridian from 70°30′N to 72°30′N in the Barents Sea (Bochkov, 1982). The data series from 1900 until 2000 has quarterly values from the period 1906–1920 and monthly values from 1921, partly measured and partly interpolated. In this presentation, the annual mean temperature is analysed.

Northeast Arctic shrimp (*P. borealis* Krøyer 1838) is located in the in the Barents Sea and near Spitsbergen at the ICES areas I and IIa in deep-water from 20 to 900 m. The data time series covers the areas East Finnmark, Tiddly Bank, Thor Iversen Bank, Bear Island Trench and Hopen from 1982 until 2001 (ICES, 2002b).

The time series of Barents Sea capelin (*M. villosus*) covers the time from 1945 to 2000. The data series of biomass from 1945 to 1995 is provided from Marshall et al. (2000), and the biomass data from 1995 to 2000 is provided by ICES (2002a). The recruitment rate is computed from 1-year recruitment (October) and spawning numbers provided from official ICES data (ICES, 2002a).

The time series of Norwegian spring spawning herring (*C. harengus*) covers the time from 1907 to 2001. The data are provided from ICES (2002b). The time series of Northeast Arctic haddock (*M. aeglefinus*) covers the period from 1950 to 2001 and they are provided from ICES (2002a).

The total time series of Northeast Arctic cod (*G. morhua*) covers the period from 1866 to 2001. The time series of from 1866 to 1900 is provided by Godø (2000). The data are interpolated from catch numbers to biomass by the scaling of 3.5 (tons/1000 numbers). The period from 1900 to 1945 is based on published estimates from Hylen (2002) and the period from 1946 to 2000 is provided by ICES (2002b).

2.2. Systems theory

The Barents Sea is a complex dynamic system of sea currents, and fluctuations in temperature, nutrients, phytoplankton, zooplankton, and fish biomasses. The system may be represented by the simplified general system model

$$S(t) = \{B(t), \{S_n(t), S_o(t), S_f(t), S_b(t), S_v(t)\}\} \quad (1)$$

where $S_n(t)$ is the lunar nodal system, $S_o(t)$ is the ocean system, $S_f(t)$ is the food chain system, $S_b(t)$ is a biomass system, $S_v(t)$ is an unknown source and $B(t)$ is the mutual binding between the Barents Sea system elements. According to the general system model, the Barents Sea is expected to be a time varying, structurally unstable, and a mutually dependent system.

The system dynamics of a biomass system $S_b(t)$ is dependent on the eigen dynamics in each system and the mutual binding $B(t)$ between the systems. If there is a stationary dominant energy cycle in one element, the cycle is expected to influence the others. In this case, the lunar nodal system $S_n(t)$ is expected to have some influence on the ocean system $S_o(t)$ and the ocean system is expected to influence the food chain to fish $S_f(t)$. The food chain $S_f(t)$ is expected to influence the biomass $S_b(t)$ of shrimp, capelin, cod, herring, and haddock in the Barents Sea. This influence may be more or less detectable dependent on the binding $B(t)$ and the disturbance $S_v(t)$.

2.2.1. The lunar nodal cycle

The Earth is influenced by planetary cycles in the time span from hours to thousands of years. A planetary cycle of special interest is the 18.6-year lunar nodal cycle. This cycle time is close to a needed planning range and it is close to life cycle of species in the Barents Sea. In this analysis, the lunar nodal system $S_n(t)$ represents gravity energy from the 18.6-year lunar nodal cycle, caused by a mutual interaction between the Earth, the Moon, and the Sun. The Moon's orbital plane changes $\pm 5°09'$ from the ecliptic plane in a cycle 18.6134 years. The maximum angle to the equatorial is $(23°27' + 5°09') = 28°36'$ and 9.3 years later, the angle is $(23°27' - 5°09') = 18°18'$. The lunar node is the cross point between the Moon plane cycle and the ecliptic plane. This cross point describes a lunar nodal cycle of 18.6134 years. The gravity energy from the Moon introduces an 18.6-year lunar nodal tide in the Atlantic Ocean and the energy introduces an 18.6-year wobbling of the Earth axis (Pugh, 1996). The orbital angle to the Moon is described by the model

$$u_0(t) = U_0 + u_0 \sin(\psi_0(t)) = U_0 + u_0 \sin(\omega_0 t + \varphi_0) \quad (2)$$

where the eccentricity $U_0 = 23°27'$. The lunar nodal cycle amplitude $u_0 = 5°09'$ (deg) and $\omega_0 = 2\pi/T_0 = 2\pi/18.6134$ (rad/year) is the lunar nodal angle frequency and t (year) is the time from $t = 1900$. The cycle amplitude of $u_0(t)$ has a maximum in November 1987 and a minimum in March 1996 (Pugh, 1996) when the phase-angle is about $\varphi_0 = 1.0\pi$ (rad).

Changes in the energy force on the Earth introduce a 18.6-year lunar nodal tide, the 18.6-year nutation of the Earth axis, and a Polar motion.

2.2.2. The ocean system

An 18.6-year lunar nodal cycle introduces an 18.6-year lunar nodal tide in the Atlantic Ocean. This lunar nodal tide may be described by the model

$$u_{\mathrm{nt}}(t) = u_{\mathrm{nt}}\sin(\Phi_{\mathrm{nt}}(t)) = u_{\mathrm{nt}}\sin(\omega_0 t + \varphi_{\mathrm{nt}}) \tag{3}$$

where the amplitude $u_{\mathrm{nt}}=3$ (cm), the nodal angle frequency $\omega_0=2\pi/T_0=2\pi/18.6134$ (rad/year) is the lunar nodal angle frequency, t (year) is the time from $t=1900$, and a phase at about $\varphi_{\mathrm{nt}}=0.5\pi$ (rad) when the tide had a maximum in January 8, 1974 (Pugh, 1996; Keeling and Whorf, 1997). This tide cycle $u_{\mathrm{nt}}(t)$ has a phase delay of about $\pi/2$ (rad) or 18.6/4 years compared to the Moon high cycle $u_0(t)$ (Eq. (2)).

The 18.6-year lunar nodal cycle is a forced energy cycle on the Earth and on-linear ocean system $S_{\mathrm{o}}(t)$. The cycle energy is then distributed as a set of harmonic and sub-harmonic cycles of tides, flow and temperature states in the ocean system. These harmonic cycles are expected to influence the Atlantic tides (Keeling and Whorf, 1997) and the Atlantic inflow to the Barents Sea. The harmonic cycles may be modelled by

$$u(t) = \sum_{n,m} u_{n,m}\sin(n\omega_{\mathrm{nt}}t/m + \varphi_{n,m}) \tag{4}$$

where $u(t)$ here is called the *lunar nodal spectrum*, $u_{n,m}$ is a cycle amplitude, m the sub-harmonic index, n the harmonic index and $\varphi_{n,m}$ the phase delay. Each harmonic cycle may then introduce a new set of harmonic cycles.

2.2.3. The biomass system

A biomass system $S_{\mathrm{b}}(t)$ has an autonomous eigen frequency that behaves like a resonance in physics. This eigen frequency is related to the maximum spawning year class (Yndestad and Stene, 2002; Yndestad, 2002). According to the general systems theory (Eq. (1)), there is a relation between all system elements. This may be modulated as a chain of events from the lunar nodal cycle $S_{\mathrm{n}}(t)$, to the ocean system $S_{\mathrm{o}}(t)$, and from the ocean system $S_{\mathrm{o}}(t)$ to biomass system $S_{\mathrm{b}}(t)$. The chain of events may be modulated by the frequency transfer function

$$x_i(j\omega) = H_i(j\omega)[u(j\omega) + v(j\omega)] \tag{5}$$

where $u(j\omega)$ represents a correlated lunar nodal spectrum, $v(j\omega)$ is non-correlated disturbance from an unknown source, $x_{\mathrm{i}}(j\omega)$ represents the frequency response in the system element $S_{\mathrm{i}}(t)$, and $H_{\mathrm{i}}(j\omega)$ represents the frequency transform function between the lunar nodal cycle and the i-te system element. In a chain of events, the mean result of a non-correlated disturbance $v(j\omega)$ is expected to have a reduced influence on $x_{\mathrm{i}}(j\omega)$. A sum of correlated stationary cycles $u(j\omega)$ is expected to amplify the influence on the element $x_{\mathrm{i}}(j\omega)$ since they have the same frequency and phase.

2.3. System identification

A stationary cycle will introduce cycles of a time variant amplitude and phase in a system element when the elements have a time variant binding $B(t)$ (Eq. (1)). In a long time series, this will introduce a time variant amplitude and phase in the estimated cycles. This property makes it difficult to identify stationary cycles by straightforward statistical methods. A second problem is that in these short time series, it is difficult to identify low frequent cycles and to separate the high frequent cycles from noise. Wavelet transformation is an appropriate method to analyse the time variant data series. A continuous wavelet spectrum is computed by the wavelet transform

$$W(a,b) = \frac{1}{\sqrt{a}}\int_R x(t)\,\Psi\left(\frac{t-b}{a}\right)\mathrm{d}t \tag{6}$$

where $x(t)$ is the analysed time series, $\Psi(\ )$ is a wavelet impulse function, $W(a,b)$ is the computed wavelet cycles, b is a translation in time and a is a time scaling parameter in the wavelet filter function. The computed wavelets $W(a,b)$ represent a set of filtered time series between the time series $x(t)$ and the impulse functions $\Psi(\ )$. In the following analysis, a Coiflet3 wavelet transform was chosen from many trials on tested data (Matlab Toobox, 1997; Daubehies, 1992). This wavelet represents a linear phase filter which is able to separate additive cycles from a time series. Computed low frequent wavelets

will have an error at the beginning and at the end of the time series. To reduce this effect, there is introduced symmetric time series by the 'sym' property in the wavelet transform (Matlab Toobox, 1997). The Kola data series is scaled by data=(data − mean(data))/sqrt(variance) to reduce the same type of error.

2.3.1. Cycle period identification

The time series $x(t)$ may be represented by a sum of dominant wavelets that has most of the energy in the time series $x(t)$. Then we have

$$x(t) = [W(k1,t) + W(k2,t) + .. + W(kn,t)] + v(t) = W(t) + v(t) \quad (7)$$

where $W(k,t)$ represents a dominant wavelet cycle and $v(t)$ is error. A wavelet cycle $W(k,t)$ represents a moving correlation to an impulse period k. A dominant cycle period thus represents the best correlation to a cycle period k and a minimum error in Eq. (7). The wavelet cycle time k is tested by computing the correlation coefficient $r(k)$ between the dominant wavelet cycle $W(k,t)$ and a potential known cycle $u(k,t)$. The correlation value of quality is computed by $q(k) = r(k)*\text{sqrt}[(n-2)/(1-r(k)*r(k))]$ where n is the number of samples. The signal to noise relation between the dominant wavelets and the error (Eq. (7)) is computed by $S/N = \text{var}(W(t))/\text{var}(x(t) - W(t)$ where k represents the dominant wavelets.

2.4. The phase-clock

Dominant stationary cycles $W(t)$ in the time series $x(t)$ (Eq. (7)), are deterministic cycles dependent on the cycle amplitude $|W(k,t)|$ and the cycle time k. A stationary cycle is represented by the model

$$W(k,t) = a(k,t)\sin(\Phi_k(t)) \quad (8)$$

where $W(k,t)$ is the cycle amplitude and $\Phi_k(t) = \omega_k t + \varphi_k$ is the rotating angle cycle. The angle frequency $\omega_k = 2\pi/k$ (rad/year) and the phase delay is φ_k.

A stationary cycle may be visualized as a vector or a phase-clock. (Fig. 1) where $a(k,t)$ represents the vector amplitude and the phase-angle $\Phi_k(t) = \omega_k t + \varphi_k$. When the time t is changing from $t = 2000$, 2001, 2002... the angle $\Phi_k(t)$ is turning in the direction from 0 to 2π and the vector is turning in an anti-clockwise direction. In biomass forecasting, the future biomass state is unknown, but the phase of the biomass fluctuation may be known. This opens a possibility of introducing a biomass forecast indicator based on a simple phase-clock.

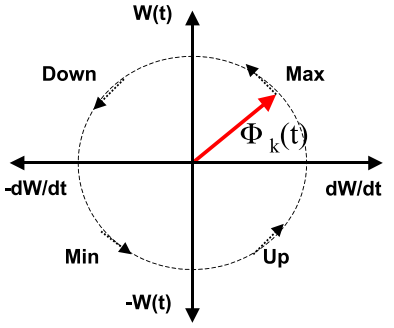

Fig. 1. The phase-clock.

3. Results

According to General System theory (Eq. (1)), there is a mutual relation between the system elements where the dominant energy source will influence the others. In this case, the lunar nodal system $S_n(t)$ is expected to influence the ocean system $S_o(t)$, the ocean system is expected to influence the food chain to fish $S_f(t)$, and the food chain to fish is expected to influence the biomass $S_b(t)$.

3.1. The Barents Sea temperature

The Barents Sea has an inflow of warm North Arctic water. This inflow meets a stream of cold Arctic water from the North and cool mixed water goes back to East Greenland. These streams may vary in intensity and slightly in position and cause biological changes in the Barents Sea. In this investigation, the Kola section temperature series $x_K(nT)$ represents an indicator of Atlantic inflow to the Barents Sea (Fig. 2).

A wavelet transform $W_{ko}(a,nT)$ of the Kola time series $x_{ko}(nT)$ has identified dominant wavelet cycles of 6, 18, 55, and 74 years. The 6-year wavelet $W_{ko}(6,nT)$ identifies temperature maximum values

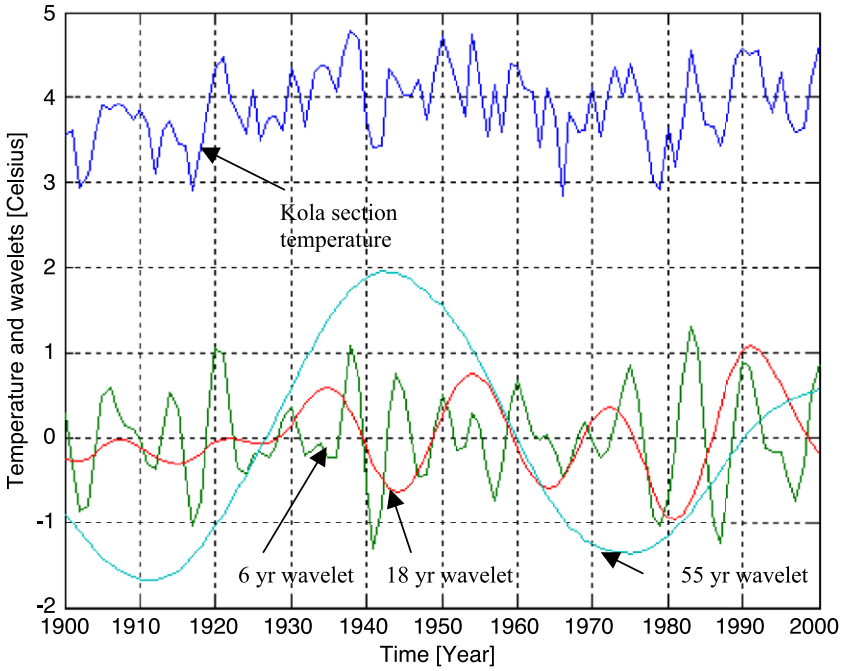

Fig. 2. Time series of Kola section data series and the 6-, 18-, and 55-year wavelet cycles.

for the years [1907 1915 1921 1930 1937 1944 1951 1961 1975 1983 1991], the 18-year wavelet $W_{ko}(18,nT)$ has maximum values in [1909 1922 1935 1955 1973 1991], the 55-year wavelet $W_{ko}(55,nT)$ has maximum values in 1945, and the 74-year wavelet $W_{ko}(74,nT)$ in 1945. A stationary model of the dominant cycles is

$$W_{ko}(06,nT) = a_{ko}(6,nT)\sin(3\omega_0 nT - 0.09\pi)$$

$$W_{ko}(18,nT) = a_{ko}(18,nT)\sin(\omega_0 nT + 0.55\pi)$$

$$W_{ko}(55,nT) = a_{ko}(55,nT)\sin(\omega_0 nT/3 + 0.90\pi) \quad (9)$$

where $\omega_0 = 2\pi/18.6134$ (rad/year), $T = 1$ year, $n = 1900...2001$, $a_{ko}(55,nT)$, $a_{ko}(18,nT)$, and $a_{ko}(06,nT)$ are time variant amplitudes. The angle $3\omega_0 nT = 0.92\pi$, $\omega_0 nT = 0.31\pi$, and $\omega_0 nT/3 = 0.85\pi$, when $n = 2001$. The estimated correlation coefficients r between the identified dominant wavelet cycles $W_{ko}(06,nT)$, $W_{ko}(18,nT)$, $W_{ko}(55,nT)$ and the estimated stationary cycles in Eq. (9) are estimated to $r_6 = 0.37$, $r_{18} = 0.88$, $r_{55} = 0.88$, and $r_{74} = 0.95$. The correlation value of quality is estimated to $q_6 = 3.9$, $q_{18} = 18.3$, $q_{55} = 30.1$ and the number of freedom $n - 2 = 98$. This gives a better than 95% confidence in a t-distribution. The signal to noise relation between the wavelets $W_{ko}(nT) = [0.4W_{ko}(06,nT) + 0.4W_{ko}(18,nT) + 0.1W_{ko}(55,nT)]$ and the estimate difference $(x_{ko}(nT) - W_{ko}(nT))$ are estimated to $S/N_{ko} = 3.2$. This confirms that the estimated nodal spectrum represents most of the fluctuations in the time series. The estimated phase-angle of the 18-year cycle is estimated to

$$\Phi_{ko}(18,nT) = \omega_0 nT + 0.55\pi = \Phi_{nt}(18,nT) + 0.05\pi \quad (10)$$

Eqs. (3) and (10) show that estimated 18-year Kola temperature cycle has the same cycle time and phase as the 18.6-year lunar nodal tide.

3.1.1. The Barents Sea temperature phase-clock

Fig. 3 shows the phase state of the dominant wavelet cycles $W_{ko}(06,nT)$, $W_{ko}(18,nT)$, and $W_{ko}(55,nT)$ at the year 2001. The 55-year cycle

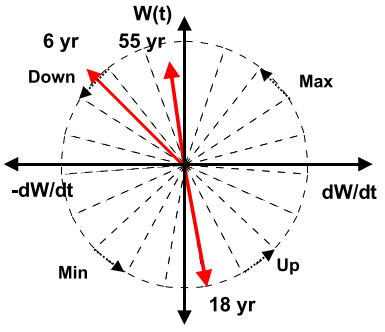

Fig. 3. The Kola section temperature phase state in the year 2001.

$W_{ko}(55,nT)$ has a maximum value, the 18-year cycle $W_{ko}(18,nT)$ has a minimum value, and the 6-year cycle $W_{ko}(06,nT)$ has passed a maximum value. This is the same maximum state as 55 years earlier in 1945.

A wavelet time series analysis of the Kola section temperature, the biomass of Northeast Arctic cod, the biomass of Barents Sea capelin, and the biomass of Norwegian Spring spawning herring show that long-term biomass growth is dependent on the phase-relation between the 6- and the 18-year temperature cycles. The biomass has a long-term growth when the two cycles are positive at the same time. There is a long-term biomass reduction when only one cycle is positive at the same time, and there is a biomass collapse when both cycles are negative at the same time (Yndestad, 2002). A phase-diagram of the cycle states may then represent a ''Temperature phase-clock'' where the cycle vectors indicate the climate state and the forecasting in cycles of 6, 18, and 55 years.

This climate clock indicates that the mean sea temperature is expected to be reduced in the next period of about 25 years. At the same time, the 18-year cycle is expected to increase the temperature the next 9 years and the 6-year cycle will decrease the temperature in the next 2 years. According to the code of long-term biomass dynamics, the 18- and the 6-year cycle are expected to be negative at the same time at about 2003. This may cause a temporary strong biomass reduction in the biomass food chain (Yndestad, 2002).

3.2. Barents Sea shrimp

Northeast Arctic shrimp (*P. borealis*) are located in the Barents Sea and near Spitsbergen and represent an important economic resource. The biomass fluctuations in local populations may change 2–105% from one year to the next (ICES, 2002a). The fluctuations are a result of the biomass growth property and environment disturbance. The growth properties of shrimp biomass have been studied for years, and it is known that water temperature has influence on the biomass recruitment, growth and mortality (Rassmussen, 1953; Teigsmark, 1980; Andersen, 1991). Other important sources of fluctuation are catching and consumption from Northeast Arctic cod and other predators.

The time series of spawning biomass of Barents Sea shrimp from 1982 until 2002 has a mean weight of age $x_{sh}(\text{age})$=[0 0 0 8 14 25 22 19 17 14] 1000 tons at the age of 1 to 10 years. Maximum spawning year class is estimated to be 25,000 tons at 6 years. The Barents Sea shrimp then have an eigen frequency at about $X_{sh}(j\omega_e)=2\pi/T_e=2\pi/6.2$ (rad/year) (Yndestad and Stene, 2002). This is the same frequency as the 6.2-year Kola temperature cycle. The biomass is then expected to follow the 6.2-year temperature cycle.

The data series $x_{sh}(nT)$ of shrimp biomass from Norwegian surveys in the Barents Sea is presented in Fig. 4. The time series cover the areas East Finnmark, Tiddly Bank, Thor Iversen Bank, Bear Island Trench and Hopen. A wavelet analysis of the shrimp biomass time series $x_{sh}(nT)$ has identified the dominant cycles of 6 and 18 years. The data series $x_{sh}(nT)$ and the identified dominant wavelet cycles $W_{sh}(6,nT)$ and $W_{sh}(18,nT)$ are shown in Fig. 4. The cross correlation coefficient between the biomass data series $x_{sh}(nT)$ and $W_{sh}(6,nT)$, $W_{sh}(18,nT)$, and $W_{sh}(nT)$=$[W_{sh}(6,nT)+W_{sh}(18,nT)]$ are estimated to $r(6)=0.45$, $r(18)=0.95$, and $r_{sh}=0.85$. The correlation value of quality is estimated to $q_{ch}=8.3$, and the number of freedom $n-2=27$. This gives a better than 95% confidence in a t-distribution. The signal to noise relation between the estimated wavelets $W_{sh}(nT)$ and the estimate difference error $(x_{sh}(nT)-W_{sh}(nT))$ are estimated to $S/N_{sh}=3.5$.

The dominant wavelet cycles $W_{sh}(06,nT)$ and $W_{sh}(18,nT)$ indicate that the dominant fluctuations of the shrimp biomass are related to the biomass eigen frequency of 6.2 years and the 18.6 years Kola temperature cycle. A stationary representation

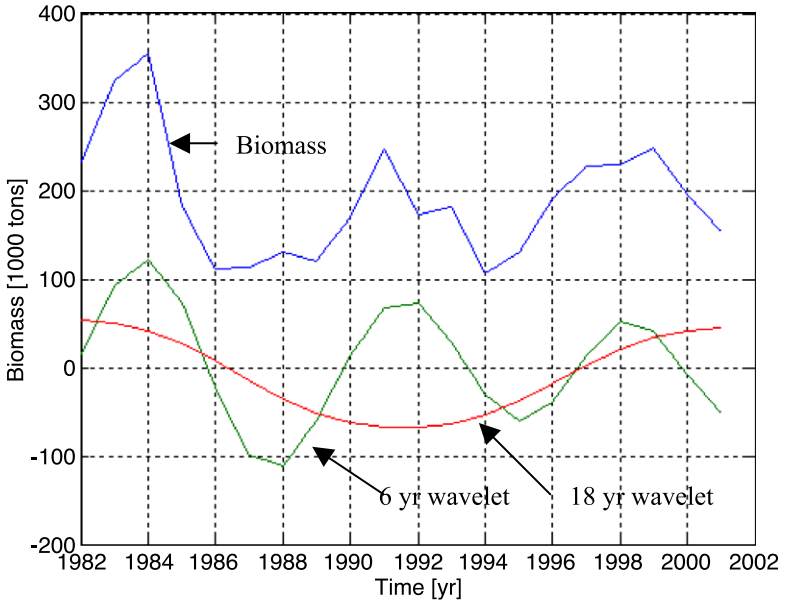

Fig. 4. The shrimp biomass from the Norwegian surveys, 6- and 18-year wavelet cycles.

of the dominant wavelet cycles is described by the model

$$W_{\mathrm{sh}}(06,nT) = 70.000\sin(3\omega_0 nT - 1.09\pi)$$

$$W_{\mathrm{sh}}(18,nT) = 30.000\sin(\omega_0 nT + 1.55\pi) \qquad (11)$$

at the years $n = 1982\ldots2001$ and sampling periods of $T = 1$ year. The cycle phase-angle of the 6- and 18-year cycle is estimated to

$$\Phi_{\mathrm{sh}}(06,nT) = 3\omega_0 nT - 1.09\pi = \Phi_{\mathrm{ko}}(06,nT) - 1.0\pi$$

$$\Phi_{\mathrm{sh}}(18,nT) = \omega_0 nT + 1.55\pi = \Phi_{\mathrm{ko}}(18,nT) - 1.0\pi \qquad (12)$$

The dominant biomass cycle has a phase delay of 1.0π (rad/year) compared to the Kola temperature cycles. This inverse relation between the shrimp biomass and the Kola temperature is explained by the additional larvae from eggs which will survive in reduced temperature.

3.2.1. The shrimp biomass phase-clock

Fig. 5 shows the state of the shrimp phase-clock at the year 2001. The 55-year cycle indicates that we may expect a long-term biomass growth the next 25 years. The 18- and the 6-year cycle have about the same state as in 1982. In a more short-term biomass growth, the 18-year cycle is expected to introduce a biomass reduction. The next 9 years, the 6-year cycle is expected to indicate a biomass growth over the first 3 years.

3.3. The Barents Sea capelin

The capelin (*M. villosus)* has a northerly circumpolar distribution. In the Atlantic, the capelin is

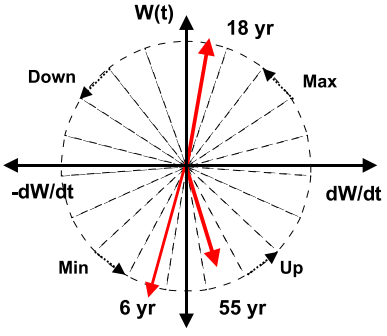

Fig. 5. The shrimp biomass phase-clock state in the year 2001.

located in the Barents Sea (ICES areas I and IIa), Iceland, Greenland, Labrador and Newfoundland. The capelin stock in the Barents Sea is the largest in the world and has maintained annual fishery catches up to 3 million tons. The capelin stock is of vital importance in the Arctic food web. It is the main plankton feeder in the area and serves as an important forage fish for other fish stocks, seals, whales and sea birds. The capelin is therefore influenced by its abiotic environment and by the abundance of food, predators, and fisheries (Gjøsæter, 1997).

The time series from 1989 until 2001 of the spawning biomass of Barents Sea capelin has a mean weight of age $x_{ca}(\text{age})$=[0 2 357 89 2] 1000 tons at the age of 1 to 5 years. Maximum spawning biomass is estimated to be 357,000 tons at 3 years (ICES, 2002a). The Barents Sea capelin then has an eigen frequency at about $X_{ca}(j\omega_e)=2\pi/T_e=2\pi/3.1$ (rad/year), which is close to the half of the 6.2-year Kola temperature cycle. This short cycle will introduce a more unstable phase in the biomass cycles and the capelin is therefore able to adapt to the growth of random fluctuations in food and predators (Yndestad and Stene, 2002).

The time series of Barents Sea capelin from 1945 until 2001 has fluctuations from about 20 to 8000 thousand tons (Fig. 6). A wavelet analysis of the time series has identified dominant wavelets cycles $W_{ca}(06,nT)$ and $W_{ca}(18,nT)$ which have cycle times of 6 and 18 years. The cross correlation coefficient between the biomass data series $x_{ca}(nT)$ and $W_{ca}(nT)=[W_{ca}(06,nT)+W_{ca}(18,nT)]$ is estimated to $r_{ca}=0.73$. The correlation value of quality is estimated to $q_{ca}=8.0$, and the number of freedom $n-2=55$. This gives a better than 95% confidence in a t-distribution. The signal to noise relation between the estimated wavelets $W_{ca}(nT)$ and the estimate difference error $(x_{ca}(nT)-W_{ca}(nT))$ is estimated to $S/N_{ca}=1.8$.

This means that the capelin biomass has harmonic dominant cycles related to the Kola temperature cycles of 6 and 18 years. The 6-year cycle is shifted to a 9-year cycle when the 18-year Kola temperature cycle has a negative state and this shift influences the phase of the 18-year cycle (Figs. 2 and 6). This important shift to a 9-year cycle is explained by a mismatch between the short biomass eigen frequency of 3.1 year and the Kola cycles influence on the recruitment rate (Yndestad and Stene, 2002). A sta-

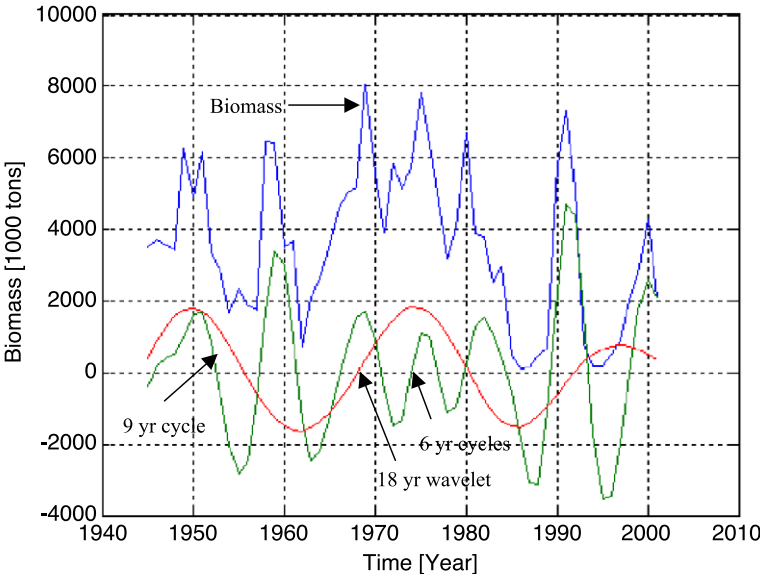

Fig. 6. The time series of Barents Sea capelin biomass from 1945 to 2001, a 18-year dominant wavelet cycle, and a dominant wavelet cycle where the cycle time changes between 6 and 9 years.

tionary representation of the dominant wavelet cycles is described by the model

$$W_{ca}(06,nT) = a_{ca}(06,nT)\sin(3\omega_0 nT - 0.09\pi)$$

$$W_{ca}(09,nT) = a_{ca}(09,nT)\sin(\omega_0 nT/2 - 0.09\pi)$$

$$W_{ca}(24,nT) = a_{ca}(24,nT)\sin(3\omega_0 nT/4 + 0.22\pi) \quad (13)$$

where $n = 1982\ldots2001$, $T = 1$ year, $W_{ca}(06,nT)$ is active when the 18-year Kola temperature is positive, and $W_{ca}(06,nT)$ is active when the 18-year Kola temperature is negative. The 24-year cycle $W_{ca}(24,nT)$ is the mean cycle of $18.6 + 6.2 = 24.8$ year. The cycle phase-angle of the 6- and 18-year cycle is estimated to

$$\Phi_{ca}(09,nT) = \omega_0 nT/2 - 1.09\pi$$

$$\Phi_{ca}(24,nT) = 3\omega_0 nT/4 + 0.22\pi \quad (14)$$

The capelin stock has an eigen frequency cycle of only 3 years. This explains the close phase-relation between the 6-year Kola cycle and the dominant biomass cycles of 6 and 9 years. The 24-year cycle has a phase delay of 0.22π (rad). This is about 3 years compared to the 18-year Kola temperature cycle. This delay is explained as a mean delay time of about 3-year growth delay in the total biomass.

3.3.1. The capelin biomass phase-clock

Fig. 7 shows the state of the Barents Sea capelin phase state at the year 2001. The 24-year cycle

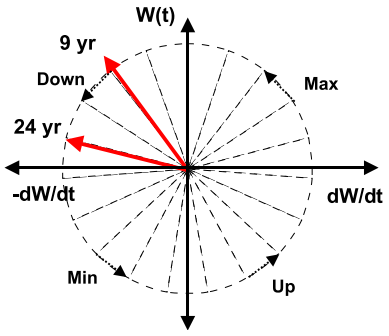

Fig. 7. The state of the Barents Sea capelin biomass phase-clock in the year 2001.

$Ws(24,nT)$ is still in a positive sector and the 9-year cycle has passed the maximum state. The climate clock indicates the same situation as in 1945. The 18-year Kola cycle is at a minimum state and the 6-year Kola cycle has passed a maximum state (Fig. 3). This will influence long-term recruitment.

In the long-term, the biomass is expected to be influenced by the relation between the 18- and the 6-year cycle during a period of 55 years in the Kola temperature cycle. The 24-year capelin biomass cycle indicates a biomass reduction the next 6 years. In a short-time range, the 9-year cycle is expected to reduce the biomass cycle the next 3–4 years, and then there is expected to be a new growth in the biomass when the 9- and the 24-year cycle turn in a positive direction.

3.4. The Norwegian spring spawning herring

The time series of Norwegian spring spawning herring (*C. harengus*) had a growth period from 5 million tons in 1920 to about 20 million tons in 1930. In the period 1950 to 1960, the biomass was reduced to 7 million tons, and in the period 1965 to 1985, there was a collapse caused by overfishing.

The spawning biomass time series of Norwegian Spring Spawning herring has a mean weight of age $x_{he}(\text{age})$=[0 0.5 14.0 94.8 37.4 569.9 561.2 428.7 332.9 281.0] thousand tons (ICES, 2002a). The mean maximum spawning biomass is 569.9 thousand tons at the age of 6 years and indicates a herring biomass eigen frequency of about $X_{he}(j\omega_e) = 2\pi/T_{he} = 2\pi/6.2$ (rad/year). This is the same cycle time as the 6.2-year Kola temperature cycle.

The wavelet analysis of the herring biomass time from 1907 to 2001 has identified the dominant wavelets cycles $W_{he}(06,nT)$, $W_{he}(18,nT)$ and $W_{he}(55,nT)$ or a cycle time of 6, 18 and 55 years (Fig. 8). The cross correlation coefficient between the biomass time series $x_{he}(nT)$ and the wavelets sum $W_{he}(nT) = [W_{he}(06,nT) + W_{he}(18,nT) + 0.4\ W_{he}(55,nT)]$ is estimated to $r_{he} = 0.92$. The correlation value of quality is estimated to $q_{he} = 23.0$, and the number of freedom $n - 2 = 93$. This gives a better than 95% confidence in a t-distribution. The signal to noise relation between the estimated wavelets $W_{ca}(nT)$ and the estimate error difference $(x_{ca}(nT) - W_{he}(nT))$ are estimated to $S/N_{sh} = 3.0$. This analysis shows the

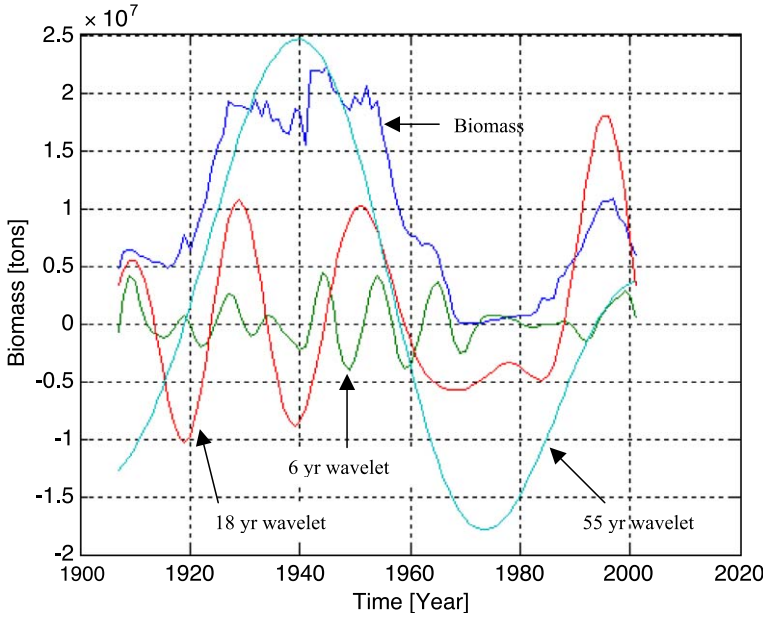

Fig. 8. Biomass of Norwegian spring spawning herring and 6-, 18- and 55-year wavelets.

biomass of Norwegian spring spawning herring is influenced by the Kola section temperature cycles of 6, 18 and 55 years. The data series and the dominant wavelet cycles are shown in Fig. 8. A stationary representation of the dominant wavelet cycles is described by the model

$$W_{\mathrm{he}}(06,nT) = a_{\mathrm{he}}(06,nT)\sin(3\omega_0 nT - 0.09\pi)$$

$$W_{\mathrm{he}}(18,nT) = a_{\mathrm{he}}(18,nT)\sin(\omega_0 nT + 1.05\pi)$$

$$W_{\mathrm{he}}(55,nT) = a_{\mathrm{he}}(55,nT)\sin(\omega_0 nT/3 + 0.90\pi) \tag{15}$$

where the year $n = 1906...2001$ and sampling periods of $T = 1$ year. The cycle phase-angle of the 6- and 18-year cycle is estimated to

$$\Phi_{\mathrm{he}}(06,nT) = 3\omega_0 nT - 0.09\pi = \Phi_{\mathrm{ko}}(06,nT) + 0.0\pi$$

$$\Phi_{\mathrm{he}}(18,nT) = \omega_0 nT + 1.05\pi = \Phi_{\mathrm{ko}}(18,nT) - 0.5\pi$$

$$\begin{aligned}\Phi_{\mathrm{he}}(55,nT) &= \omega_0 nT/3 + 0.90\pi \\ &= \Phi_{\mathrm{ko}}(55,nT) + 0.0\pi\end{aligned} \tag{16}$$

The estimated 6-year cycle has the same frequency and phase as the 6-year Kola temperature cycle. This close phase-relation is explained by a biomass eigen frequency cycle of about 6 years. Maximum recruitment will then follow the temperature cycle. The 18-year cycle has a delay of $\pi/2$ (rad) compared to the 18-year Kola temperature cycle. This confirms that the 18-year Kola cycle controls the long-term biomass growth (Yndestad, 2002). The estimated 55-year biomass cycle has the same frequency and phase as the 55-year Kola temperature cycle. This indicates that both cycles represent a mean of the 6- and the 18-year cycles.

3.4.1. The herring biomass phase state

Fig. 9 shows the phase state of Norwegian spring spawning herring biomass phase-clock in the year 2001. This corresponds to the same state as in 1945. The 55-year cycle state shows that we may expect a mean long-term biomass reduction the next 25 years. This indicated that the biomass has reached a maximum state. In 1945, the herring biomass was about 20 million tons, and in 1997, the biomass was about 10 million tons. The difference in the maximum biomass in 1945 and 2001 may be explained by the 1970 collapse in the biomass and the short period

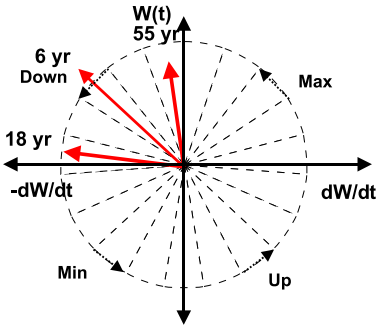

Fig. 9. The state of Norwegian spring spawning herring biomass phase-clock in the year 2001.

of biomass growth from the 1980s when the 55-year Kola cycle started to turn in a positive direction. In a short-term of 6 years, the biomass is expected to be reduced the next 3 years when the 6-year cycle is turning in a negative direction. The medium-term cycle of 18 years is expected to introduce a new growth period of 9 years when the 18-year Kola cycle goes into a positive state.

3.5. The northeast arctic cod

Northeast Arctic cod (*G. morhua*) is the largest stock of *G. morhua* cod in the world. The fishery of this stock is located along the northern coast of Norway and in the Barents Sea. For centuries, this stock of cod has been the most important economic biomass for Norwegian fisheries and of vital importance for settlement and economic growth in the western part of Norway. The biomass of Northeast Arctic cod has always fluctuated. In the wavelet analysis, we will identify the source of dominant cycles in the time series.

The time series $x_{co}(nT)$ of Northeast Arctic cod spawning biomass has a mean weight of age $x_{co}(\text{age})$= [0 201 6078 20341 65,388 103,012 93,124 63,528 41,586 13,932] tons from age 1 until 10 (ICES, 2002b). In this estimate, the maximum biomass is 103,012 tons at the age of 6 years. From this age distribution, we may conclude that the cod biomass has an eigen frequency at about $X_{co}(j\omega_e) = 2\pi/T_{co} = 2\pi/6.2$ (rad/year).

Fig. 10 shows the time series $x_{co}(nT)$ of Northeast Arctic cod from 1866 until 2001 (Godø, 2000; ICES, 2002b). The wavelet analysis of the cod biomass time from 1866 to 2000 has identified the dominant wavelets cycles $W_{co}(06,nT)$, $W_{co}(18,nT)$ and $W_{co}(55,nT)$ or a cycle time of 6, 18 and 55–75 years (Fig. 10). The 55-year cycle is a dominant cycle, but is influenced by short connected time series and the biomass collapse in the 1980s. The cross correlation coefficient be-

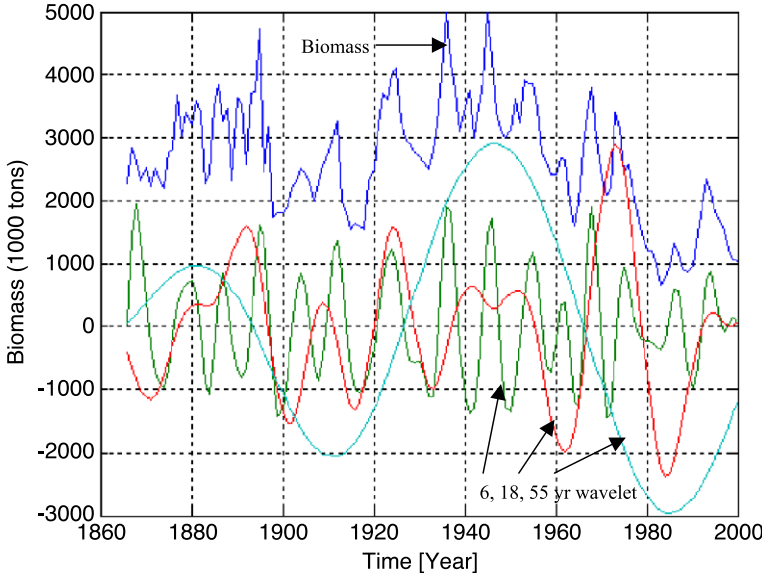

Fig. 10. Time series of Northeast Arctic cod and dominant wavelet cycles of 6, 18, and 55 years.

tween the biomass time series $x_{co}(nT)$ and the wavelets sum $[W_{co}(06,nT)+W_{co}(18,nT)+W_{co}(55,nT)]$ is estimated to $r_{co}=0.85$. The correlation value of quality is estimated to $q_{he}=18.6$, and the number of freedom $n-2=133$. This gives a better than 95% confidence in a t-distribution. The signal to noise relation between the estimated wavelets $W_{co}(nT)=[0.7W_{co}(06,nT)+0.5W_{co}(18,nT)+0.3W_{co}(55,nT)]$ and the estimate difference $(x_{co}(nT)-W_{co}(nT))$ is estimated to $S/N_{co}=3.8$.

The dominant wavelet cycle indicates that most fluctuations of the Northeast Arctic cod biomasses are related to the 6.2-year biomass eigen frequency and the Kola temperature cycle of 6.2, 18.6 and 55.8 years. In this estimate, the 55-year wavelet estimate is influenced by the collapse in 1980 (Yndestad, 2002). A stationary representation of the dominant wavelet cycles is described by the model

$$W_{co}(6,nT)=a(6,nT)\sin(3\omega_0 nT-1.09\pi)$$

$$W_{co}(18,nT)=a(18,nT)\sin(\omega_0 nT+0.22\pi)$$

$$W_{co}(55,nT)=a(55,nT)\sin(\omega_0 nT+0.72\pi) \qquad (17)$$

in the years $n=1866...2001$ and sampling periods of $T=1$ year. The cycle phase-angle of the 6 and 18-year cycle is estimated to

$$\Phi_{co}(06,nT)=3\omega_0 nT-1.09\pi=\Phi_{ko}(06,nT)+1.0\pi$$

$$\Phi_{co}(18,nT)=\omega_0 nT+0.22\pi=\Phi_{ko}(18,nT)-0.33\pi$$

$$\Phi_{co}(55,nT)=\omega_0 nT/3+0.72\pi=\Phi_{ko}(55,nT)+0.18\pi \qquad (18)$$

This shows that the cod biomass has dominant cycles which are closely related to the Kola temperature cycle. The 6-year cycle $W_{co}(06,nT)$ has a delay of π (rad) or 3 years compared to the 6-year Kola temperature cycle $W_{ko}(06,nT)$. This represents a delay of 3 years which is the delay for the time when the Kola cycle introduces maximum recruitment to the first 3-year class in the biomass. The 18-year cycle $W_{co}(18,nT)$ has a delay of 0.33π (rad) or 3 years compared to the 18-year Kola temperature cycle. The $W_{co}(55,nT)$ cycle delay of 0.18π (rad) or about 6 years is the delay to maximum biomass in the eigen frequency cycle.

3.5.1. The cod biomass phase-clock

Fig. 11 shows the state of Northeast Arctic cod biomass phase-clock at the years 2001. The phase-clock has about the same state as in 1945. The 55-year Kola cycle is expected to introduce a long-term mean biomass reduction in a period of about 25 years. In short-term forecasting, the 6-year cycle in expected to introduce a biomass reduction the next 3 years. At this state, there is a critical period that may introduce a collapse in the biomass. In 6 years, the 18-year cycle will turn in a positive direction and introduce a positive state the next 9 years.

3.6. The northeast arctic haddock

Northeast Arctic haddock (*M. aeglefinus*) is a bottom fish found at a depth of 130–1.000 ft. Its most important spawning grounds are off Mid Norway, Southwest Iceland and the Faroe Islands. Little is known about the migratory patterns of haddock. The young haddock is located in the Barents Sea while the larger haddock tend to migrate south. Some spawning migration occurs along the coast of Northern Norway, whereafter it migrates back to the Barents Sea. Most haddock fishing is coastal, but in the North, fishing also takes place in the eastern reaches of the Norwegian Economic Zone.

The spawning biomass time series of Northeast Arctic haddock has a mean age weight vector x_{ha}

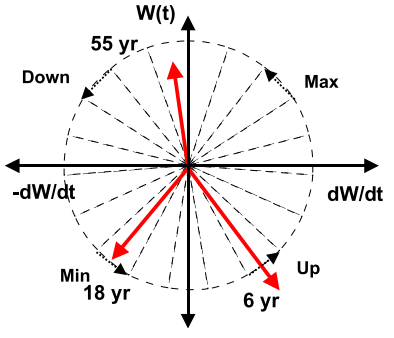

Fig. 11. The state of Northeast Arctic cod biomass phase-clock in the year 2001.

(age)=[0 0 1 7 14 16 12 6 1.5] million tons (ICES, 2002b). The maximum biomass is 16 million tons at the age of 6 years, and identifies a haddock biomass eigen frequency of about $X_{ha}(j\omega_e)=2\pi/T_{ha}=2\pi/6.2$ (rad/year). This is close to the same cycle time as the 6.2-year Kola section temperature cycle.

The time series of Northeast Arctic haddock has the same fluctuations as the Northeast Arctic cod. In the period 1950 to 1975, the biomass was reduced from about 4 million to about 2 million tons, and in first part of the 1990s, there was a temporary increase in of the biomass. A wavelet analysis of the time series has identified dominant wavelets cycles $W_{ha}(06,nT)$ and $W_{ha}(18,nT)$ or cycle time of 6 and 18 years.

The wavelet analysis of the haddock biomass time from 1950 to 2001 has identified the dominant wavelets cycles $W_{ha}(06,nT)$, $W_{ha}(18,nT)$ or a cycle time of 6 and 18 years (Fig. 12). The cross correlation coefficient between the biomass time series $x_{co}(nT)$ and the wavelets sum $[W_{ha}(06,nT)+W_{ha}(18,nT)]$ is estimated to $r_{ha}=0.80$. The correlation value of quality is estimated to $q_{ha}=9.4$, and the number of freedom $n-2=49$. This gives a better than 95% confidence in a t-distribution. The signal to noise relation between the estimated wavelets $W_{ha}(nT)=[W_{ha}(06,nT)+0.5W_{ha}(18,nT)+0.5W_{ha}(55,nT)]$ and the estimate difference is estimated to $S/N_{ha}=6.5$. The data series and the dominant wavelet cycles are shown in Fig. 12. A stationary representation of the dominant wavelet cycles is described by the model

$$W_{ha}(06,nT)=a(06,nT)\sin(3\omega_0 nT-1.09\pi)$$

$$W_{ha}(18,nT)=a(18,nT)\sin(\omega_0 nT+0.22\pi) \qquad (19)$$

at the years $n=1950\ldots2001$ and sampling periods of $T=1$ year. The cycle phase-angle of the 6- and 18-year cycle is estimated to

$$\Phi_{ha}(06,nT)=3\omega_0 nT-1.09\pi=\Phi_{ko}(06,nT)-1.0\pi$$

$$\Phi_{ha}(18,nT)=\omega_0 nT+0.22\pi=\Phi_{ko}(18,nT)-0.33\pi \qquad (20)$$

The 18-year cycle $W_{ha}(18,nT)$ and the 6-year cycle $W_{ha}(06,nT)$ have a delay of about 3 years compared to the Kola temperature cycles. The same delay is estimated in the cod biomass.

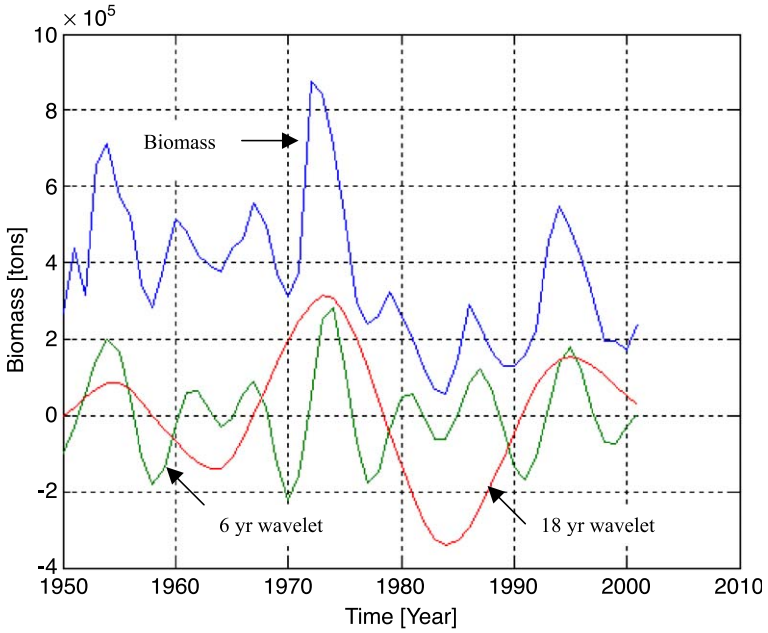

Fig. 12. Time series of Northeast Arctic haddock and dominant wavelet cycles of 6 and 18 years from 1950 to 2001.

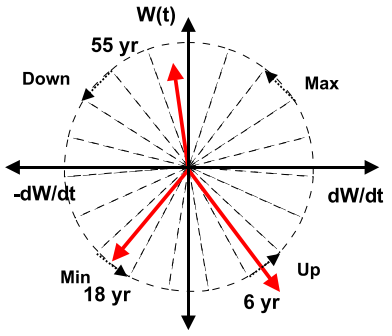

Fig. 13. The state of the Northeast Arctic haddock biomass phase-clock in the year 2001.

3.6.1. The haddock biomass phase-clock

Fig. 13 shows the state of Northeast Arctic haddock biomass phase-clock in 2001. The phase-clock has about the same state as Northeast Arctic cod. The time series is too short to estimate a 55-year cycle, but the 55-year Kola cycle is expected to introduce the same long-term biomass reduction as in the cod biomass. In a short-term forecasting, the 6-year cycle is expected to introduce a biomass growth over the next 2 years, but at the same time, the 18-year cycle will introduce a biomass reduction the next 6 years. In 2005–2006, both cycles are expected to be at a minimum state at the same time. In this state, there is a critical period that may introduce a collapse in the biomass. From 2005–2006, the 18-year cycle is expected to turn in a positive direction and the biomass is expected to grow the next 9 years.

4. Discussion

The biomass dynamics in the Barents Sea is a result of many mutual interactions between the ocean system, the food chain, catch, and a multi-species system (Eq. (1)). A long-term biomass management is based on the theory that if we are able to forecast the biomass dynamics, then we may control the biomass. In this investigation, there is a dominant lunar nodal spectrum identified in all analysed time series. Since the lunar nodal spectrum has a stationary cycle time, it opens a new possibility for a long-term forecasting.

The Newton approach of forecasting by difference equations represents a ballistic view of the reality. By this simple approach, it is difficult to separate natural biomass fluctuations from estimate errors. This problem introduces a short forecast period and it may lead to an instability in biomass management (Yndestad, 2001). The holistic Aristotle approach of forecasting represents a rotary or cycle view of the reality. This analysis indicates that there is a chain of reactions from the lunar nodal cycle to the biomass dynamics in the Barents Sea. This process may be understood as a chain of oscillators where gravity from the Moon is the forced oscillator and where energy is distributed on the Earth. The Earth energy is distributed in the chain of coupled oscillators in ocean tides, the food chain, and the biomasses in the Barents Sea. The stationary cycles in oscillating systems may be represented as vectors or a phase-clock. By this method, we may forecast when the biomass fluctuations are expected to change directions.

4.1. The Kola section temperature

The Kola section temperature series is an indicator of Atlantic inflow to the Barents Sea. It is generally believed that inflow of Atlantic water to the Barents Sea is driven by atmospheric conditions (Loeng et al., 1997). The identified dominant lunar nodal spectrum indicates that Atlantic inflow is influenced by the lunar nodal tide. Long period tides have been identified in the Atlantic Ocean and in the Barents Sea (Pettersson, 1914, 1915, 1930). Maksimov and Smirnov (1965) have analysed the surface temperature in the North Atlantic and found estimated temperature cycles close to the 18.6-year nutation cycle. The 18.6-year nodal tide has a pole-ward velocity component (Maksimov and Smirnov, 1967) and an amplitude that is approximately 7% of the lunar diurnal component. This will influence the surface layer ocean and air temperature at high latitudes (Royer, 1993; Keeling and Whorf, 1997). Maksimov and Smirnov have suggested there is a long period tide in the Barents Sea (Maksimov and Smirnov, 1964, 1967; Maksimov and Sleptsov-Shevlevich, 1970; Yndestad, 1999a). A wavelet analysis of Polar motion, Barents Sea ice extent, the NAO winter index indicates the Earth nutation introduces a nodal spectrum of about $18.6/15 = 1.2$, $18.6/3 = 6.2$, 18.6 and $4*18.6 = 74.5$ years in the Polar motion. The same spectrum is identified in Barents Sea ice extent and in the NAO winter index (Yndestad, 2003). This anal-

ysis indicates that the 6.2-, 18.6- and 74.5-year cycles are caused by a push–pull effect between the Atlantic Ocean and the Arctic Ocean where circulating water in the Arctic Ocean is influenced by Polar motion. A possible source of the 55.8-year cycle is an additive relation between the 6.2- and the 18.6-year cycle.

4.2. The food chain dynamics

Fluctuations in Atlantic inflow to the Barents Sea influence fluctuations in the sea temperature, the ice extent, the air temperature, the light conditions, the nutrients, the phytoplankton biomass, and the zooplankton biomass. *Calanus finmarchicus* is a major component in fuelling the recruitment and growth of capelin, herring and cod in the Barents Sea. Investigations show that there is strong correlation between Atlantic inflow and the growth of the *C. finmarchicus* zooplankton (Sundby, 2000). Total zooplankton density, dominated by the copepod (*C. finmarchicus*) is almost three times higher in the Atlantic water, than in melt water (Hassel et al., 1991; Melle and Skjoldal, 1998). This probably explains the high growth during warm periods. The density of plankton in the largest size fraction is significantly higher in colder Arctic water than in the eastern areas of the Barents Sea (Melle and Skjoldal, 1998). An analysis of zooplankton time from 1987 to 2001 shows there is a close relation between the Kola temperature cycles of 6.2 and 18.6 years, fluctuations in the zooplankton time series and the capelin recruitment rate (Yndestad and Stene, 2002).

4.3. The biomass dynamics

The estimated relation between biomass cycles and temperature cycles support the matching theory from Johan Hjort on a macro-level. Hjort (1914) analysed the length distribution of Northeast Arctic cod and explained fluctuations in the biomass as caused by a match or mismatch between the spawning time and food for the larvae.

The biomass dynamics of Northeast Arctic shrimp, Norwegian Spring spawning herring, Northeast Arctic cod, and Northeast Arctic haddock have an eigen frequency cycle of abort 6.2 years. The Barents Sea capelin has an eigen frequency cycle of about 6.2/2 years. If we look at the biomasses as a set of resonators, there will be an optimal recruitment when there is a match between the 6.2-year Kola temperature cycle and the 6-year biomass resonator cycle time. A more close analysis of long-term herring fluctuations shows that there is a long-term growth when the 6.2- and the 18.6-year cycles are positive at the same time, a biomass reduction when they are not, and a biomass collapse when both cycles are negative (Yndestad, 2002). This property explains estimated long-term fluctuations in the biomass of capelin, cod and herring in the Barents Sea (Izhevskii, 1961, 1964; Ottestad, 1942; Wyatt et al., 1994; Yndestad, 1999b; Malkov, 1991, 2002).

4.4. Methods and materials

The analysis has some potential sources of errors. There may be errors in the data samples which cannot be controlled. In this investigation, long trends in the data are analysed. Changes in methods of estimating data may then influence the long-term cycles. There is a potential source of a long-term error in long-term fluctuations between connected time series. The herring time series has a connection in 1946, the cod time series in 1900 and 1946. This may have influenced the phase of the estimated dominant cycles. The computed wavelets represent a low-pass filtered data series. Single random data errors are not therefore supposed to be a major problem in the wavelet analysis.

The time series is analysed by a wavelet transformation to identify dominant cycle periods and phase relations. The Coiflet3 wavelet transformation (Matlab Toobox, 1997) is chosen from many trials on tested data. This wavelet transformation is useful to identify cycles in the time series. The cycle identification has two fundamental problems. One problem is identifying periodic cycles when the phase has a reversal in the time series. The phase reversal property of the stationary cycles excludes traditional spectrum estimate methods. The problem is solved by first identifying the dominant cycles and correlates the cycles to known reference cycles. The second problem is identifying the long period cycles of 55 and 74 years. This problem is solved by the same method. First, identify the dominant long wavelet periods, then correlate the periods to a known cycle reference.

The results have identified good correlation between the time series and the dominant wavelet cycles, and there is good correlation between the dominant wavelet cycles and the lunar nodal spectrum. There is good correlation between the time series and the estimated dominant wavelet cycles, and there is a good signal to noise relation between the estimated wavelets and the noise difference. The close relation between the lunar nodal tide cycles and the biomass eigen frequency in all biomasses supports the indication of a long-term adopted property. The 18.6-year Kola section temperature cycle has a stationary frequency but not always a stationary phase. This property may influence the Kola temperature phase-clock. A closer analysis of the Kola section temperature series and Barents Sea ice extent has identified that the phase of the 18.6-year temperature cycle has shifted 180° in the period from about 1890 until 1925 when a 74-year was in a negative state (to be published). The phase reversal of the lunar nodal cycles explains why this cycle has been difficult to identify by others (Ottersen et al., 2000).

4.4.1. The implications

The results show a close relation between the stationary 18.6-year lunar nodal tide, dominant temperature cycles in the Barents Sea, and dominant cycles in the biomass of Barents Sea shrimp, Barents Sea capelin, Norwegian Spring spawning herring, Northeast Arctic cod, and Northeast Arctic haddock. This opens a new perspective to describe time variant climate dynamics and biomass dynamics in the Barents Sea. The deterministic property of the cycles opens a new set of possibilities for better forecasting and long-term management. The deterministic relation between biomass growth and the Kola cycles opens a possibility of more optimal management in short-term periods of 6 years, medium-term management of 18 years and long-term management of 55–75 years. The phase-clock is a simple indicator of the current state of the biomass. This will help fisheries and the industry to make better plans for the future.

Acknowledgements

I would like to thank Vladimir Ozhigin at PINRO institute in Murmansk and Svein Sundby at Institute of Marine Research (IMR) in Bergen for access to the Kola section temperature data series, Olav Rune Godø at IMR in Bergen for access to the data series on Northeast Arctic cod and Tara Marshall at IMR in Bergen for access to the Barents Sea capelin data series.

References

Andersen, P.J., 1991. Age, growth and mortality of the nothern Shrimps *Pandalus borealis* Krøyer in Pavlof Bay, Alaska. Fishery Bulletin, vol. 89. US Dept. of Commerce, National Oceanic and Fishery. Washington D.C., pp. 541–553.

Bochkov, Y.A., 1982. Water temperature in the 0–200 m layer in the Kola–Meridian in the Barents Sea, 1900–1981Sb. Nauchn. Trud., vol. 46. PINRO, Murmansk, pp. 113–122 (in Russian).

Daubehies, I., 1992. Ten lectures of wavelet. SIAM Journal on Mathematical Analysis 24 (2), 499–519. Mar. 1993.

Gjøsæter, H., 1997. Studies of the Barents Sea capelin, with emphasis on Growth. Dr scient thesis, Department of Fisheries and Marine Biology, University og Bergen, Norway, Paper III, IV and V.

Godø, O.R., 2000. Fluctuation in Stock Properties of Arco-Norwegian Cod Related to Long-term Environmental Changes. IIASA. Interim Report IR-00-023. April 6, 2000 Austria. http://www.iiasa.ac.at/cgi-bin/pubsrch?IR00023.

Hassel, A., Skjoldal, H.R., Gjøsæter, H., Omli, L., 1991. Impact of grazing from capelin (*Mallotus villosus*) on zooplankton: a case study in the northern Barents Sea in August 1985. Polar Research 10 (2), 371–388.

Hjort, J., 1914. Fluctuations in the Great Fisheries of Northern Europe Andr. Fred. Høst and Files, Copenhagen April.

Hylen, A., 2002. Fluctuations in abundance of Northeast Arctic cod during the 20th century. ICES Marine Science Symposia, 543–550.

ICES, 2002a. Northern Pelagic and Blue Whiting Fisheries Working Group. ICES CM 2002/ACFM:19. Vigo Spain. 29 Aril–8 May. 2002.

ICES, 2002b. Report of the Arctic Fisheries Working Group. ICES CM 2002/ACFM:18. ICES Headquarters 16–25 April 2002.

Izhevskii, G.K., 1961. Oceanological Principles as Related to the Fishery Productivity of the Seas Pishcepromizdat, Moscow [Translated 1966: Israel Program for Science Transactions. Jerusalem]. 95 pp.

Izhevskii, G.K., 1964. Forecasting of oceanological conditions and the reproduction of commercial fish. All Union Science Research Institute of Marine Fisheries and Oceanography. Israel Program for Science Transactions, Jerusalem. 22 pp.

Keeling, C.D., Whorf, T.P., 1997. Possible forcing global temperature by oceanic tides. Proceedings, National Academy of Science of the United States 94, 8321–8328 (August).

Loeng, H., Ozhigin, V., Ådlandsvik, B., 1997. Water fluxes through the Barents Sea. ICES Journal of Marine Science 54, 310–317.

Maksimov, I.V., Smirnov, N.P., 1964. Long range forecasting of secular changes of the general ice formation of the Barents

Sea by the harmonic component method. Murmansk Polar Sci. Res. Inst., Sea Fisheries 4, 75–87.

Maksimov, I.V., Smirnov, N.P., 1965. A contribution to the study of causes of long-period variations in the activity of the Gulf Stream. Oceanology 5, 15–24.

Maksimov, I.V., Smirnov, N.P., 1967. A long-term circumpolar tide and its significance for the circulation of ocean and atmosphere. Oceanology 7, 173–178 (English edition).

Maksimov, I.V., Sleptsov-Shevlevich, B.A., 1970. Long-term changes in the tide-generation force of the moon and the iciness of the Arctic Seas. Procedings of the N.M. Knipovich Polar Scientific-Research and Planning Institute of Marine Fisheries and Oceanography (PINRO) 27, 22–40.

Malkov, A.S., 1991/L. Movement of the earth pole and population dynamics of some commercial fish species from the northern Atlantic. The 79th international ICES Annual Science Symposium. ICES, Copenhagen, p. 77.

Malkov, A.S., 2002. Movements of the Earth pole and population dynamics of Norwegian Spring spawning herring and Arctic cod. The 90'th International ICES Annual Science Symposium, Copenhagen, Denmark, 1 Oct-5. CM 2002/O:09.

Marshall, T.C., Yaragina, N.A., Ådlandsvik, B., Dolgov, A.V., 2000. Reconstruction the stock–recruit relationship for Northeast Arcric cod using a bioenergetic index of reproductive potential. Canadian Journal of Fisheries and Aquatic Sciences 57, 2433–2442.

Matlab Toobox, 1997. Users Guide. The Math Works, 24 Prime Park Way, Natick, USA.

Melle, W., Skjoldal, H.R., 1998. Distribution, life cycle and reproduction of *Calanus finmarchicus*, *C, hyperboreus* and *C. Glacialis* in the Barents Sea. Dr scient thesis, Department of Fisheries and Marine Biology, University og Bergen, Norway, Paper III. 33 pp.

Ottersen, G., Ådlandsvik, B., Loeng, H., 2000. Predicting the temperature of the Barents Sea. Fisheries Oceanography 9 (2), 121–135.

Ottestad, P., 1942. On periodical variations on the yield on the great sea fisheries and the possibility of establishing yield prognoses. Fiskeridirektoratets Skrifter VII (5) (Bergen, Norway).

Pettersson, O., 1914. Climatic variations in historic (*sic*) and prehistoric time. Svenska Hydrogr. Biol. Kommissiones Skrifter 5, 26.

Pettersson, O., 1915. Long periodical (*sic*) variations of the tide-generating force: Conseil Permanente International pour l'Exploration de la Mer (Copenhagen). Pub. Circ. 65, 2–23.

Pettersson, O., 1930. The tidal force. A study in geophysics. Geografiska Annaler 18, 261–322.

Pugh, D.T., 1996. Tides, Surges and Mean Sea-Level. Wiley, New York.

Rassmussen, B., 1953. On the geographical variation in growth and sexual development of deep sea prawn (*Pandalus borealis* Kr.). Fiskeridir. Skr. Havundersøkelser. 10 (3), 1–160 (160 p. Bergen. Norway).

Rollefsen, G., Strøm, J., et al. 1949. NORSK FISKERI OG FANGST HÅNDBOK. BIND 1. Alb. Cammermeyers Forlag. Oslo. Norway (in Norwegian).

Royer, T.C., 1993. High-latitude oceanic variability associated with the 18.6-Yr nodal tide. Journal of Geophysical Research 98 (C3), 4639–4644 (March 15).

Sundby, S., 2000. Recruitment of Atlantic cod stocks in relation to temperature and advection of copepod populations. *Sarsia* 85, 277–298.

Teigsmark, G., 1980. Populasjoner av dyphavsreke (*Pandalus borealis* Krøyer i Barentshavet, Universitetet i Bergen. Norway.

Wyatt, T., Currie, R.G., Saborido-Ray, F., 1994. Deterministic signals in Norwegian cod records. ICES Marine Science Symposium 198, 49–55.

Yndestad, H., 1999a. Earth nutation influence on the temperature regime in the Barents Sea. ICES Journal of Marine Science 56, 381–387.

Yndestad, H., 1999b. Earth nutation influence on system dynamics of Northeast arctic cod. ICES Journal of Marine Science 56, 562–657.

Yndestad, H., 2001. Earth nutation influence on Northeast Arctic management. ICES Journal of Marine Science 58, 799–805.

Yndestad, H., 2002. . The 2002 ICES Annual Science Conference. Copenhagen. "The Code of Long-term Fluctuations of Norwegian Spring spawning herring". CM 2002/Q:02.

Yndestad, H., 2003. A lunar nodal spectrum in Arctic time series. ICES Annual Science Conference. Sept 2003. Tallinn. ICES CM 2003/T. ICES. Copenhagen.

Yndestad, H., Stene, A., 2002. System dynamics of Barents Sea Capelin. ICES Journal of Marine Science 59, 1155–1166.